**Table of Contents**

# Additional Figures and Tables



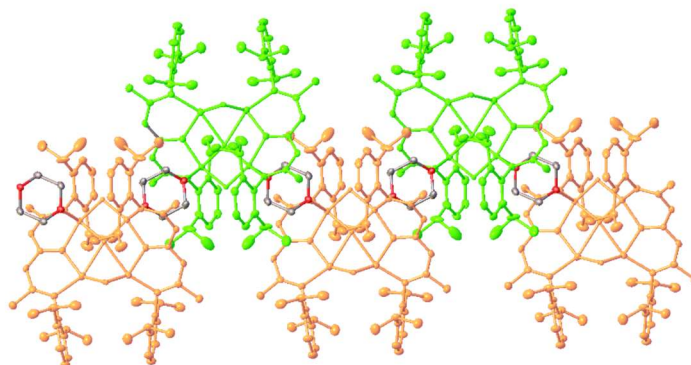**Figure S1.** Solid-state structure of **(BODDI)₂(MgH)₄_a** (hydrogen atoms except the hydrides are omitted for the sake of clarity) in view along the a-axis. Adjacent molecules bridged by 1,4-dioxane are given in green and orange, respectively.



**Figure S2.** Solid-state structure of **(BODDI)₂(MgH)₄_a** (hydrogen atoms except the hydrides are omitted for the sake of clarity) in view along the b-axis. Adjacent molecules bridged by 1,4-dioxane are given in green and orange, respectively.



**Figure S3.** Solid-state structure of **(BODDI)₂(MgH)₄_a** (hydrogen atoms except the hydrides are omitted for the sake of clarity) in view along the c-axis. Adjacent molecules bridged by 1,4-dioxane are given in green and orange, respectively.
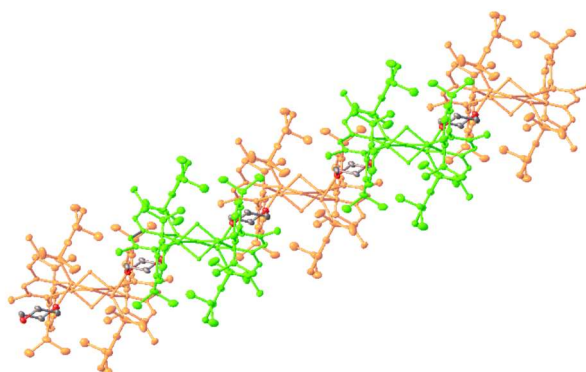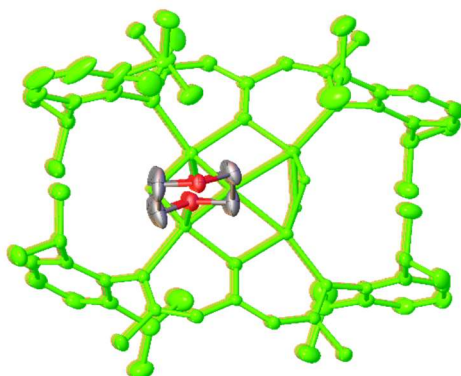
**Figure S4.** Solid-state structure of **(BODDI)₂(MgH)₄_b** (hydrogen atoms except the hydrides are omitted for the sake of clarity) in view along the a-axis. Adjacent molecules bridged by 1,4-dioxane are given in green and orange, respectively.



**Figure S5.** Solid-state structure of **(BODDI)₂(MgH)₄_b** (hydrogen atoms except the hydrides are omitted for the sake of clarity) in view along the b-axis. Adjacent molecules bridged by 1,4-dioxane are given in green and orange, respectively.
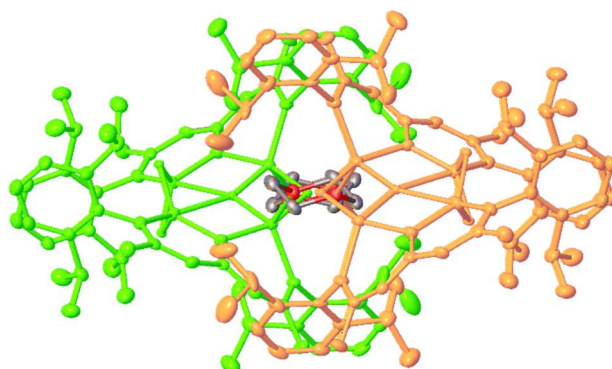


**Figure S6.** Solid-state structure of **(BODDI)₂(MgH)₄_b** (hydrogen atoms except the hydrides are omitted for the sake of clarity) in view along the c-axis. Adjacent molecules bridged by 1,4-dioxane are given in green and orange, respectively.
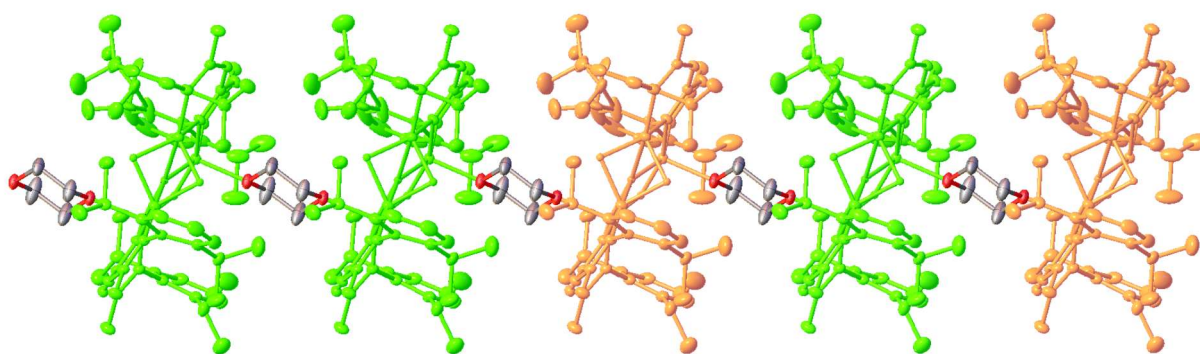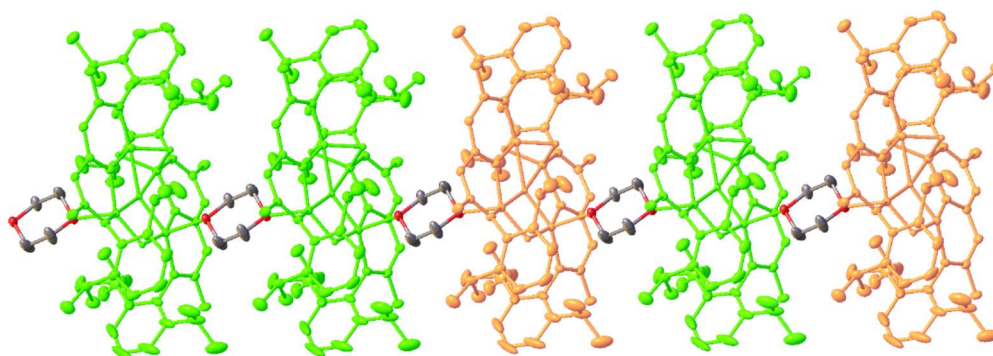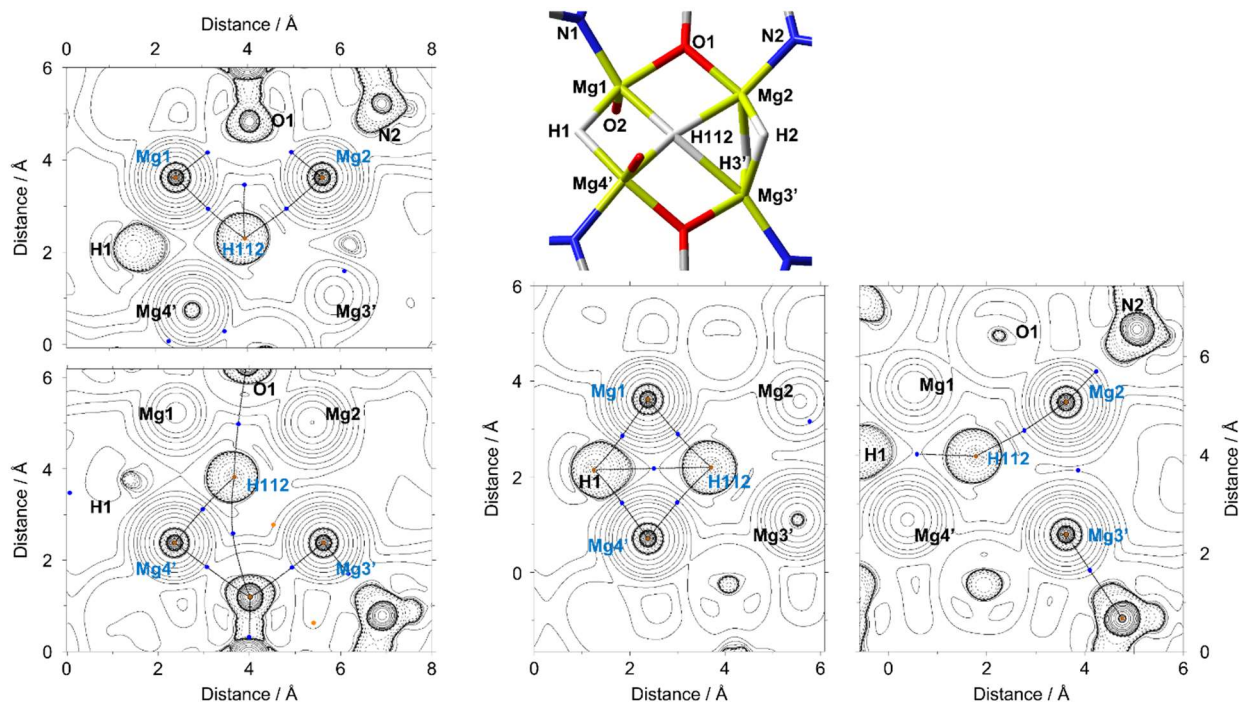
**Figure S7.** Topology of the electronic bonds in the vicinity of the $\mu_4$-hydride of **(BODDI)$_2$(MgH)$_4$_b** as given by NBO analysis. Atoms highlighted in blue define the respective plane, bond and ring critical points are shown in dark blue and orange, respectively, bond paths in black.

**Table S1.** Selected structural properties such as bond lengths ($d$ in Å), bond angles ($\alpha$ in °) and dihedral angles ($\delta$ in °) in the vicinity of the tetranuclear magnesium hydride cluster of **(BODDI)$_2$(MgH)$_4$_b** as obtained at the DFT level of theory in solution (toluene); see Figure 2 for labels.

| $d$ / Å | | $\alpha$ / ° | | $\delta$ / ° | |
|---|---|---|---|---|---|
| Mg1-H1 (Mg2-H1) | 1.840 (1.866) | Mg1-H1-Mg4' | 103.6 | Mg1-Mg2-Mg3'-Mg4' | 19.9 |
| Mg1-H112 (Mg4'-H112) | 1.998 (1.948) | Mg1-H112-Mg4' | 95.1 | Mg1-Mg4'-Mg3'-Mg2 | 21.6 |
| Mg2-H112 (Mg3'-H112) | 2.134 (2.426) | Mg2-H2-Mg3' | 91.0 | | |
| Mg2-H2 (Mg3'-H3') | 1.886 (1.863) | Mg2-H112-Mg3' | 71.9 | | |
| Mg2-H3'(Mg3'-H2) | 1.924 (1.883) | N1-Mg1-O1 | 89.4 | | |
| Mg1-N1 | 2.076 | N1-Mg1-O2 | 104.3 | | |
| Mg1-O1 | 2.018 | N2-Mg2-O1 | 90.5 | | |
| Mg1-O2 | 2.097 | | | | |
| Mg2-N2 | 2.071 | | | | |
| Mg2-O1 | 1.997 | | | | |

**Table S2.:** Selected atomic charges in the vicinity of the tetranuclear magnesium hydride cluster of **(BODDI)$_2$(MgH)$_4$_b** as obtained using by natural bond order analysis (NBO) as well as based on an atoms in molecules charge analysis (Bader); see Figure 2 for labels.

| | NBO | AIM |
|---|---|---|
| Mg1 | 1.717 | 1.707 |
| Mg2 | 1.683 | 1.689 |
| Mg3' | 1.682 | 1.684 |
| Mg4' | 1.722 | 1.707 |
| H1 | -0.800 | -0.793 |
| H2 | -0.804 | 0.797 |
| H3' | -0.807 | -0.797 |
| H112 | -0.857 | -0.831 |
| O1 | -1.028 | -1.412 |
| O2 | -0.715 | -1.150 |
| N1 | -0.850 | 1.411 |
| N2 | -0.823 | -1.422 |

**Table S3.:** Selected Wiberg bond indices (WBIs) in the vicinity of the tetranuclear magnesium hydride cluster of **(BODDI)$_2$(MgH)$_4$_b** as obtained using by natural bond order analysis (NBO); see Figure 2 for labels. WBIs for Mg–H bonds are represented by a bold font type.

|       | Mg1      | Mg2      | Mg3'     | Mg4'     | N1   | N2   | O1   | O2   | H1   | H2   | H3'  | H112 |
|-------|----------|----------|----------|----------|------|------|------|------|------|------|------|------|
| Mg1   |          |          |          |          |      |      |      |      |      |      |      |      |
| Mg2   | 0.01     |          |          |          |      |      |      |      |      |      |      |      |
| Mg3'  | 0.00     | 0.03     |          |          |      |      |      |      |      |      |      |      |
| Mg4'  | 0.02     | 0.00     | 0.01     |          |      |      |      |      |      |      |      |      |
| N1    | 0.07     | 0.00     | 0.00     | 0.00     |      |      |      |      |      |      |      |      |
| N2    | 0.00     | 0.09     | 0.00     | 0.00     | 0.02 |      |      |      |      |      |      |      |
| O1    | 0.05     | 0.07     | 0.00     | 0.00     | 0.07 | 0.02 |      |      |      |      |      |      |
| O2    | 0.05     | 0.00     | 0.00     | 0.00     | 0.00 | 0.00 | 0.00 |      |      |      |      |      |
| H1    | **0.15** | 0.01     | 0.00     | **0.14** | 0.00 | 0.00 | 0.00 | 0.00 |      |      |      |      |
| H2    | 0.00     | **0.14** | **0.13** | 0.00     | 0.00 | 0.00 | 0.00 | 0.00 | 0.00 |      |      |      |
| H3'   | 0.00     | **0.11** | **0.15** | 0.00     | 0.00 | 0.00 | 0.00 | 0.00 | 0.00 | 0.02 |      |      |
| H112  | **0.07** | **0.04** | **0.02** | **0.08** | 0.00 | 0.00 | 0.01 | 0.00 | 0.01 | 0.00 | 0.01 |      |

**Table S4.:** 2e-stabilization energy ($\Delta E_{ij}^{(2)}$) orbital energy difference ($\varepsilon_j - \varepsilon_i$) and overlaps ($F_{ij}$) between the $i^{\text{th}}$ donor NBO of H112 (LP$_i$; $q_i$ = 1.86) and the $j^{\text{th}}$ acceptor NBO of the respective Mg atom (LP$_j^*$) for **(BODDI)$_2$(MgH)$_4$_b**; see Figure 2 for labels.

| Donor | Acceptor | $\Delta E_{ij}^{(2)}$ / kJ·mol$^{-1}$ | $\varepsilon_j - \varepsilon_i$ / a.u. | $F_{ij}$ / a.u. |
|-------|----------|------------------------------|-------------------------------|---------------|
| H112  | Mg1      | 96.8                         | 0.40                          | 0.088         |
| H112  | Mg2      | 64.8                         | 0.36                          | 0.069         |
| H112  | Mg3'     | 37.5                         | 0.36                          | 0.052         |
| H112  | Mg4'     | 103.1                        | 0.40                          | 0.091         |

## Experimental Procedures

### General considerations

All preparations were performed under an inert atmosphere of dinitrogen by means of Standard Schlenk-line techniques, while the samples for analytics were handled in a glovebox (GS-Systemtechnik and MBraun). Yields are not optimized and refer to isolated crystalline material. Toluene was used as p.a. grade and distilled from Na/benzophenone prior to use. $C_6D_6$ was dried over molecular sieves prior to use. The protio-ligand **(BODDI)H₂** and diethyl magnesium dioxane adduct were prepared according to literature procedure.[1]

### Characterization

The NMR spectra were recorded with a Bruker Avance 400 spectrometer with $\delta$ referenced to external tetramethylsilane ($^1$H and $^{13}$C). $^1$H and $^{13}$C NMR spectra were calibrated by using the solvent residual peak ($C_6D_5H$: $\delta(^1H)$ = 7.16) and the solvent peak ($C_6D_6$: $\delta(^{13}C)$ = 128.39), respectively. IR spectra (given in cm$^{-1}$) were recorded with an Agilent Cary 630 FT-IR spectrometer using a diamond ATR unit.

### Synthetic procedures

Synthesis of **(BODDI)(MgEt)₂**: A Schlenk-flask equipped with a stir bar was charged with (BODDI)H₂ (1,0 g, 2.17 mmol, 1 equiv.) and 20 mL toluene under inert conditions. A suspension of Et₂Mg(dx)₂ (1.235 g, 4.78 mmol, 2.2 equiv.) in 20 mL toluene was added dropwise at 0 °C. The solution was stirred at room temperature over night. The product crystallizes from the reaction mixture at room temperature as fine needles (860 mg, 51%). $^1$H NMR (400 MHz, $C_6D_6$): δ = -0.17 [q, 4H, $J$ = 8.26 Hz, Mg-C$H_2$-CH₃], 1.25 - 1.23 [m, 6H, Mg-CH₂-C$H_3$], 1.29 [d, $J$ = 6.72 Hz, 12H, CH(C$H_3$)₂], 1.38 [d, $J$ = 7.02 Hz, 12H, CH(C$H_3$)₂], 1.63 [s, 6H, C$H_3$], 3.29 [sept, $J$ = 6.72 Hz, 4H, C$H$(CH₃)₂], 3.62 [s, 16H, $dx$], 4.82 [s, 2H, γ-C$H$], 7.20 [s, 6H, $Ar$]. $^{13}$C NMR (100 MHz, $C_6D_6$) δ = -2.75 [Mg$C$H₂CH₃], 13.73 [MgCH₂$C$H₃], 24.35 [$C$H₃], 24.74 [CH($C$H₃)₂], 25.16 [CH($C$H₃)₂], 28.67 [$C$H(CH₃)₂], 67.94 [$dx$], 94.48 [γ-$C$H], 124.25 [$m$-$C$H$_{arom}$], 125.86 [$p$-$C$H$_{arom}$], 142.8 [$o$-$C_{arom}$], 145.65 [$i$-$C_{arom}$], 168.63 [$C$N], 174.37 [$C$O]; IR(ATR): ṽ = 3055, 2961, 2926, 2864, 2825, 1530, 1456, 1435, 1381, 1366, 1310, 1297, 1256, 1217, 1167, 1120, 1100, 1064, 995, 965, 936, 919, 891, 872, 850, 831, 816, 796, 775, 762, 738, 697, 677 cm$^{-1}$; Elemental analysis calculated (found) $C_{43}H_{68}Mg_2N_2O_5$: C 69.64 (68.17), H 9.24 (9.31), N 3.78 (3.60).

Synthesis of **(BODDI)₂(MgH)₄**: A Schlenk-flask equipped with a stir bar was charged with **BODDI(MgEt)₂** (1,0 g, 1.238 mmol, 1 equiv.) and 50 mL toluene under inert conditions. PhSiH₃ (0.66 mL, 5.393 mmol, 4 equiv.) was added and the solution was stirred at 80°C over night. The reaction mixture was filtered and the solvent removed under reduced pressure, resulting in a viscous oil. The product crystallized at room temperature and was washed with a small amount of hexane (158 mg, 21%). $^1$H NMR (400 MHz, $C_6D_6$): δ = 1.04 [d, 24H, $J$ = 6.72 Hz, CH(C$H_3$)₂], 1.10 [d, 24H, $J$ = 6.72 Hz, CH(C$H_3$)₂], 1.57 [s, 12H, C$H_3$], 3.17 [sept, 8H, C$H$(CH₃)₂], 3.41 [s, 8H, $dx$], 3.66 [s, 4H, Mg-$H$], 4.96 [s, 4H, γ-C$H$], 7.06 - 7.14 [m, 12H, $Ar$]. $^{13}$C NMR (75 MHz, $C_6D_6$) δ = 24.59 [CH($C$H₃)₂], 24.72 [CH($C$H₃)₂], 25.26 [$C$H₃], 28.39 [$C$H(CH₃)₂], 67.78 [$dx$], 94.42 [γ-$C$H], 124.15 [$m$-$C$H$_{arom}$], 125.42 [$p$-$C$H$_{arom}$], 143.48 [$o$-$C_{arom}$], 145.77 [$i$-$C_{arom}$], 169.22 [$C$N], 174.99 [$C$O]; IR(ATR): ṽ = 3056, 2960, 2924, 2866, 1534, 1463, 1454, 1431, 1379, 1310, 1273, 1256, 1211,

1167, 1122, 1100, 1064, 1053, 995, 978, 924, 891, 872, 846, 831, 794, 762, 753, 725, 708, 693 cm$^{-1}$; Elemental analysis calculated (found) $C_{66}H_{96}Mg_4N_4O_4$: C 71.63 (70.79), H 8.74 (9.05), N 5.06 (4.64).

## Crystallographic details

The intensity data for the compounds were collected on a Nonius KappaCCD diffractometer using graphite-monochromated Mo-K$_\alpha$ radiation. Data were corrected for Lorentz and polarization effects; absorption was taken into account on a semi-empirical basis using multiple-scans.[2-4] The structures were solved by direct methods (SHELXS)[5] and refined by full-matrix least squares techniques against Fo$^2$ (SHELXL-2018)[6]. All hydride ions were located by difference Fourier synthesis and refined isotropically; the other hydrogen atoms were included at calculated positions with fixed thermal parameters. All non-hydrogen atoms were refined anisotropically.[6] Olex2 was used for structure representations and ellipsoids are displayed at 50% probability.[7]

*Crystal Data for* **(BODDI)$_2$(MgH)$_4$_a**: $C_{73}H_{104}Mg_4N_4O_4$, $M_r$ = 1198.84 g mol$^{-1}$, colourless prism, size 0.112 x 0.092 x 0.088 mm, monoclinic, space group C 2/c, a = 18.6792(8), b = 26.1398(13), c = 15.8494(6) Å, $\beta$ = 112.900(2)°, V = 7128.9(5) Å$^3$ , T= -140 °C, Z = 4, $\rho_{calcd.}$ = 1.117 gcm$^{-3}$, µ (Mo-K$_\alpha$) = 0.99 cm$^{-1}$, multi-scan, trans$_{min}$: 0.6392, trans$_{max}$: 0.7456, F(000) = 2600, 22101 reflections in h(-22/22), k(-31/31), l(-17/19), measured in the range 1.417° $\leq \Theta \leq$ 25.681°, completeness $\Theta_{max}$ = 99.8%, 6771 independent reflections, R$_{int}$ = 0.1092, 4892 reflections with F$_o$ > 4$\sigma$(F$_o$), 404 parameters, 0 restraints, R1$_{obs}$ = 0.0858, wR2$^2_{obs}$ = 0.1784, R1$_{all}$ = 0.1270, wR2$^2_{all}$ = 0.1961, GOOF = 1.207, largest difference peak and hole: 0.318 / -0.361 e Å$^{-3}$.

*Crystal Data for* **(BODDI)$_2$(MgH)$_4$_b**: $C_{66}H_{96}Mg_4N_4O_4$, $M_r$ = 1106.70 g mol$^{-1}$, light yellow prism, size 0.092 x 0.064 x 0.062 mm, triclinic, space group P $\bar{1}$, a = 8.6237(2), b = 16.2380(4), c = 23.7002(7) Å, $\alpha$ = 104.510(1), $\beta$ = 97.671(1), $\gamma$ = 91.644(2)°, V = 3177.48(14) Å$^3$ , T= -140 °C, Z = 2, $\rho_{calcd.}$ = 1.157 gcm$^{-3}$, µ (Mo-K$_\alpha$) = 1.06 cm$^{-1}$, multi-scan, trans$_{min}$: 0.6928, trans$_{max}$: 0.7456, F(000) = 1200, 40474 reflections in h(-11/11), k(-21/21), l(-30/30), measured in the range 1.375° $\leq \Theta \leq$ 27.482°, completeness $\Theta_{max}$ = 99.4%, 14414 independent reflections, R$_{int}$ = 0.0423, 10820 reflections with F$_o$ > 4$\sigma$(F$_o$), 769 parameters, 1 restraints, R1$_{obs}$ = 0.0736, wR2$^2_{obs}$ = 0.1413, R1$_{all}$ = 0.1045, wR2$^2_{all}$ = 0.1571, GOOF = 1.098, largest difference peak and hole: 0.555 / -0.368 e Å$^{-3}$.

**Supporting Information available:** Crystallographic data (including structure factors) has been deposited with the Cambridge Crystallographic Data Centre as supplementary publication CCDC-2250664 for **(BODDI)$_2$(MgH)$_4$_a**, and CCDC-2250665 for **(BODDI)$_2$(MgH)$_4$_b**. Copies of the data can be obtained free of charge on application to CCDC, 12 Union Road, Cambridge CB2 1EZ, UK [E- mail: deposit@ccdc.cam.ac.uk].
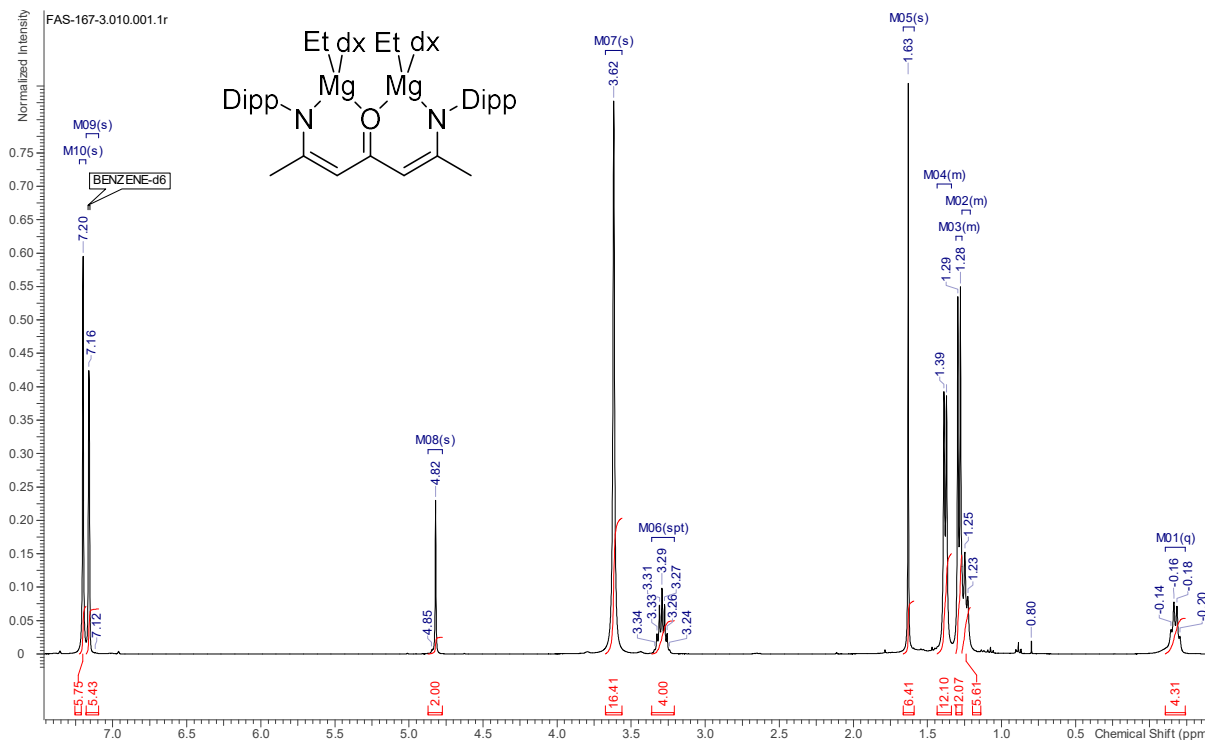
# NMR and IR spectra



**Figure S8.** $^1$H NMR spectrum (400 MHz) of **(BODDI)(MgEt)$_2$*dx$_2$** in C$_6$D$_6$ (solvent peak at 7.16 ppm).
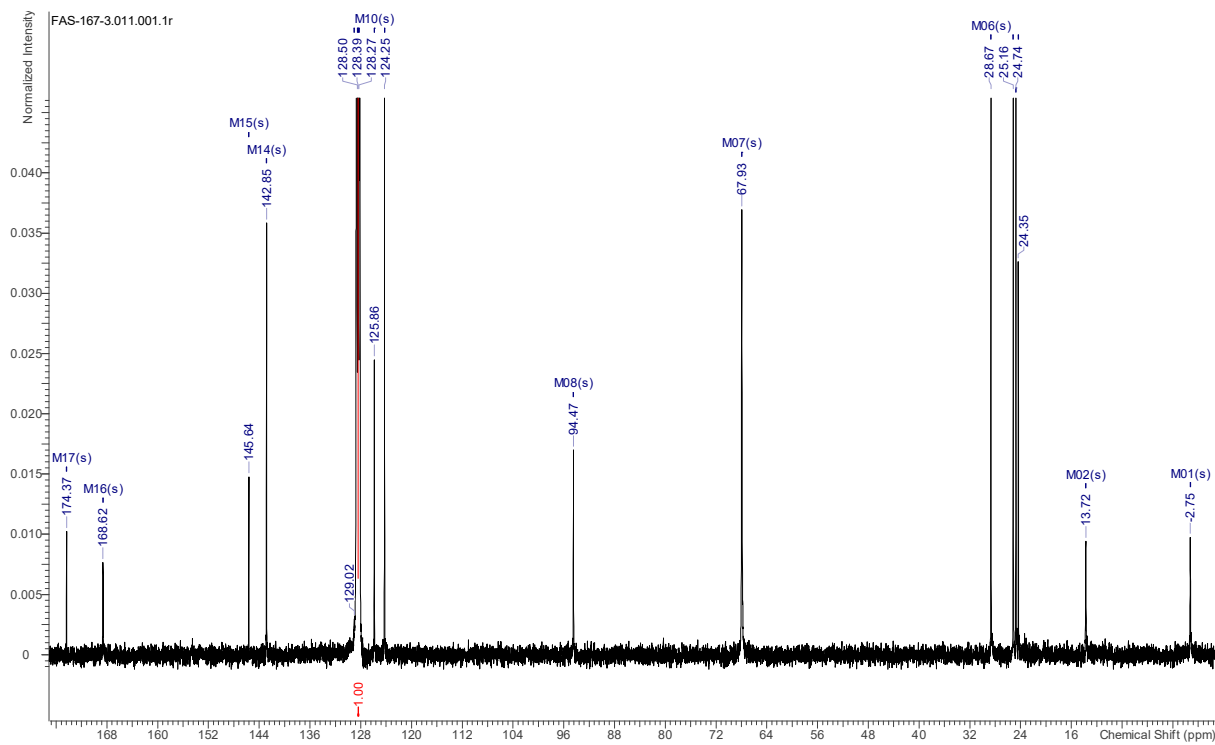


**Figure S9.** $^{13}$C NMR spectrum (101 MHz) of **(BODDI)(MgEt)$_2$*dx$_2$** in C$_6$D$_6$ (solvent peak at 128.39 ppm).

9
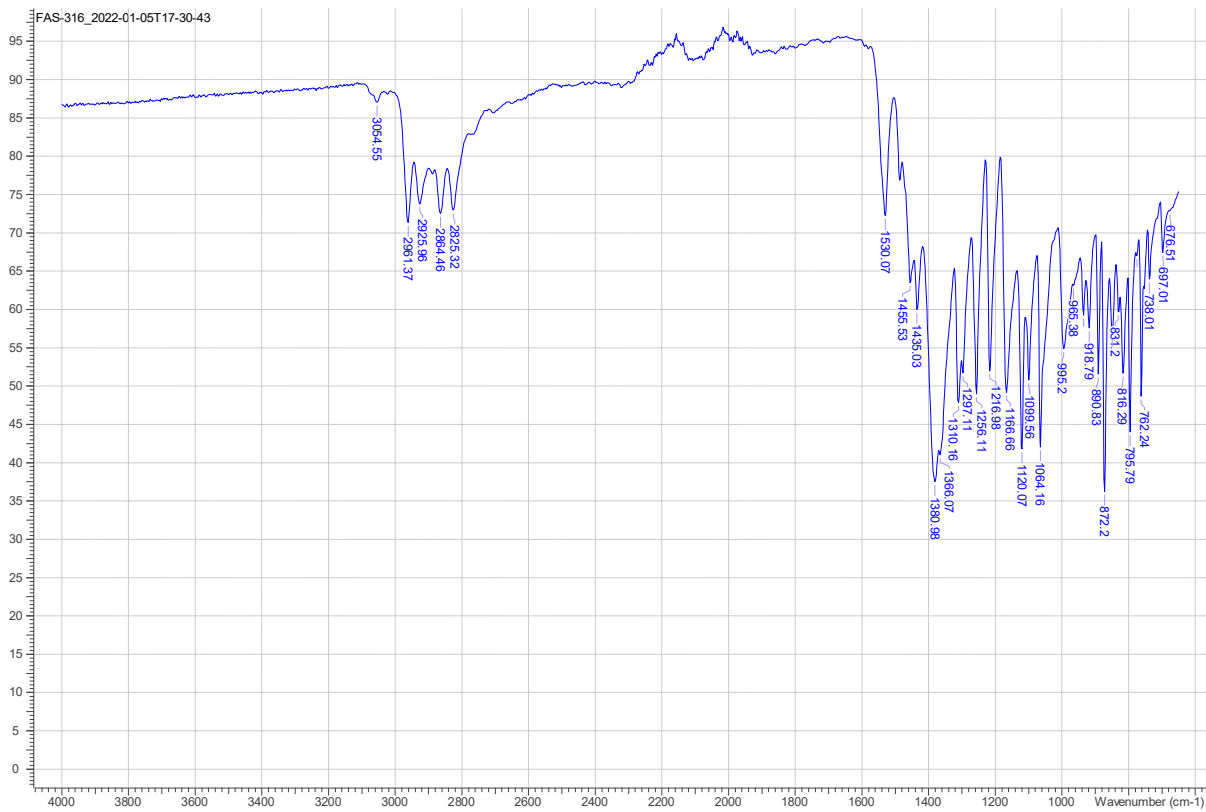
**Figure S10.** ATR-IR (diamond) spectrum of **(BODDI)(MgEt)$_2$*dx$_2$**.

**Figure S11.** $^1H$ NMR spectrum (400 MHz) of **(BODDI)₂(MgH)₄*dx** in $C_6D_6$ (solvent peak at 7.16 ppm).



**Figure S12.** $^{13}C$ NMR spectrum (75 MHz) of **(BODDI)₂(MgEt)₂*dx₂** in $C_6D_6$ (solvent peak at 128.39 ppm).
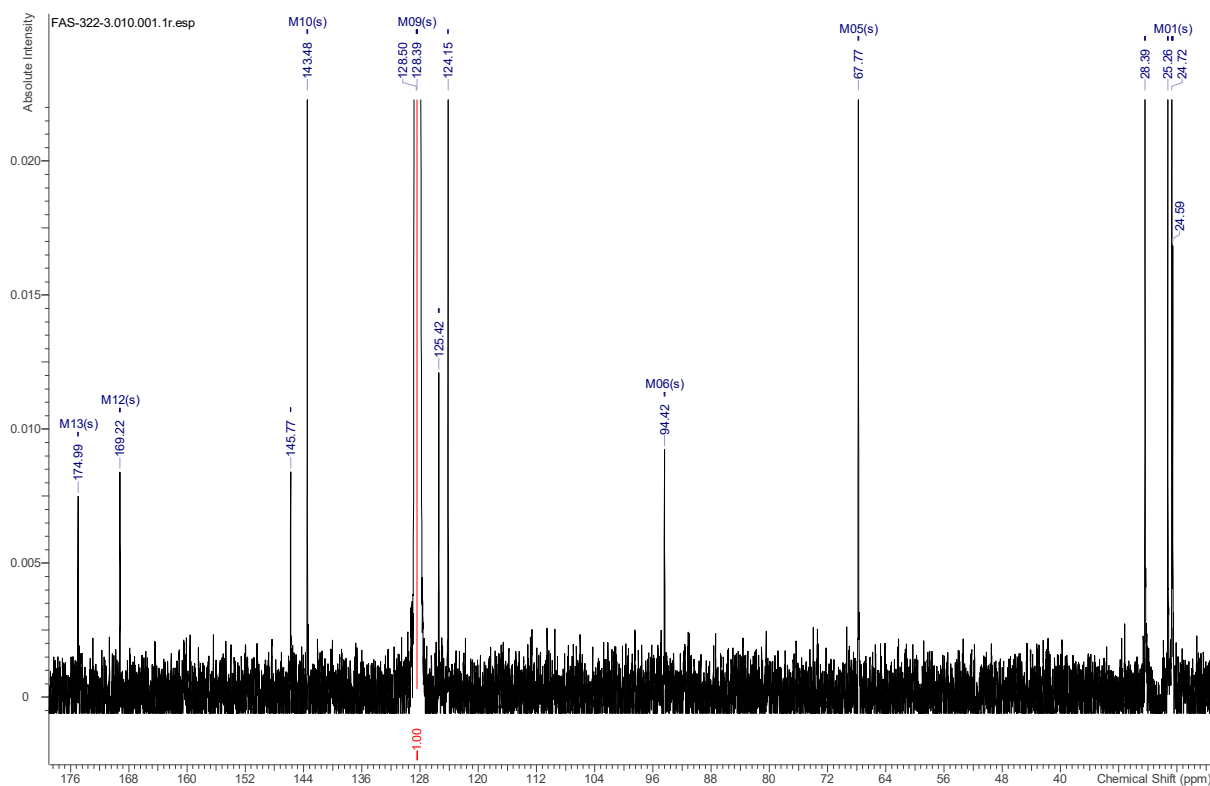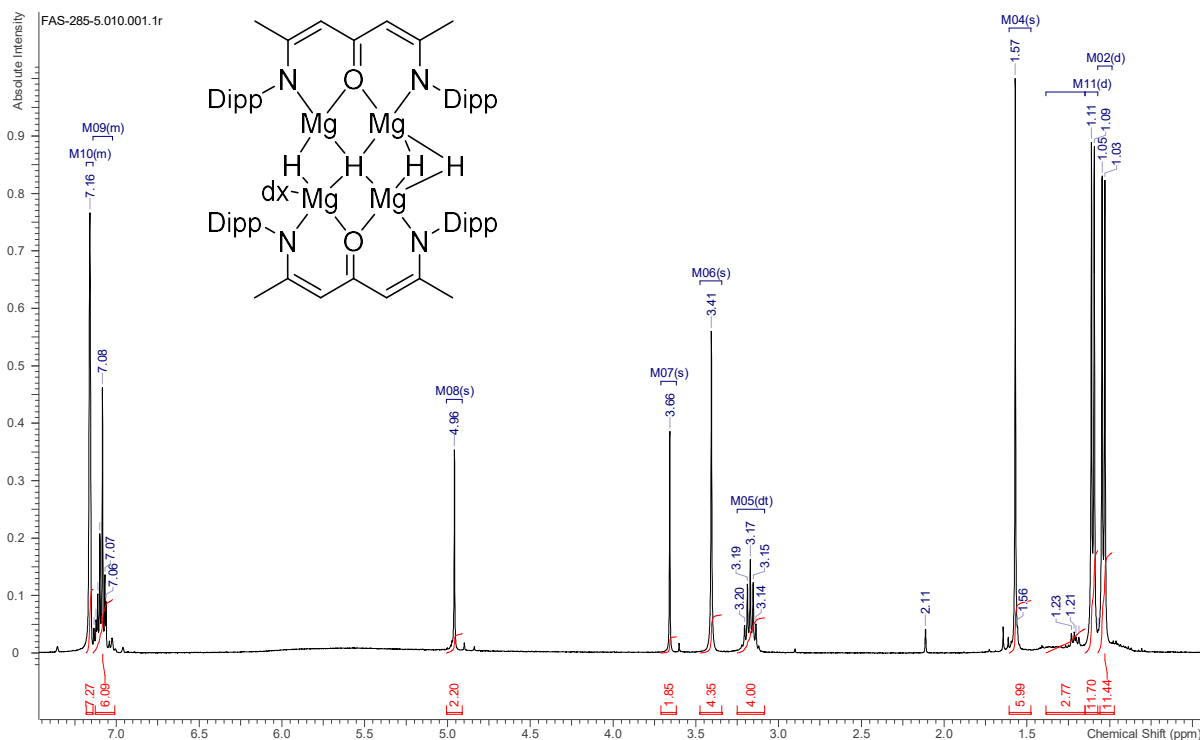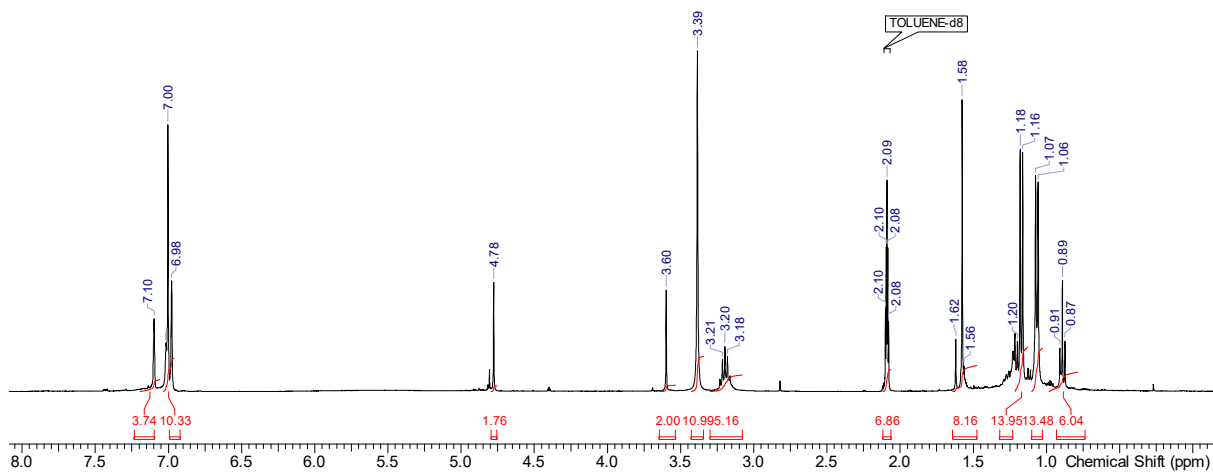
**Figure S13.** $^1$H NMR spectrum (400 MHz) of **(BODDI)(MgEt)₂*dx₂** in toluene-d₈ (solvent peaks at 2.09, 6.98, 7.00, and 7.09 ppm) at 297 K.
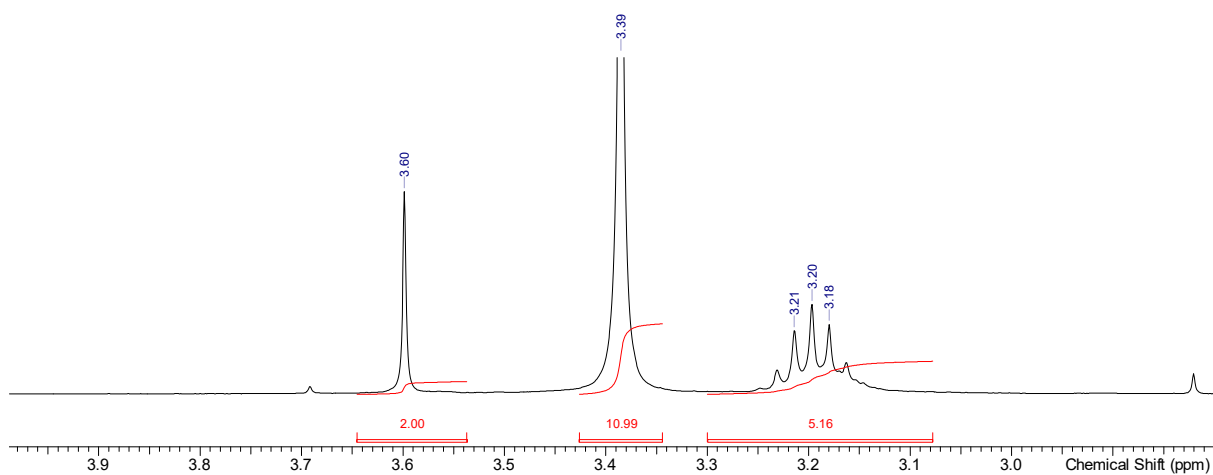


**Figure S14.** Selected region of the $^1$H NMR spectrum (400 MHz) of **(BODDI)(MgEt)₂*dx₂** in toluene-d₈ (solvent peaks at 2.09, 6.98, 7.00, and 7.09 ppm) at 297 K.
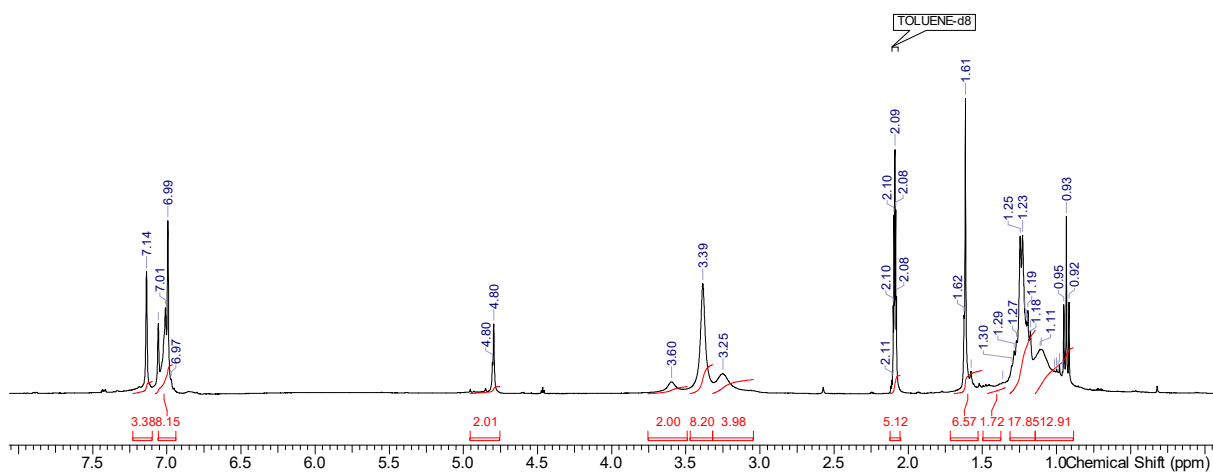


**Figure S15.** $^1$H NMR spectrum (400 MHz) of **(BODDI)(MgEt)₂*dx₂** in toluene-d₈ (solvent peaks at 2.09, 6.98, 7.00, and 7.09 ppm) at 233 K.

12

**Figure S16.** Selected region of the $^1$H NMR spectrum (400 MHz) of **(BODDI)(MgEt)$_2$*dx$_2$** in toluene-d$_8$ (solvent peaks at 2.09, 6.98, 7.00, and 7.09 ppm) at 233 K.
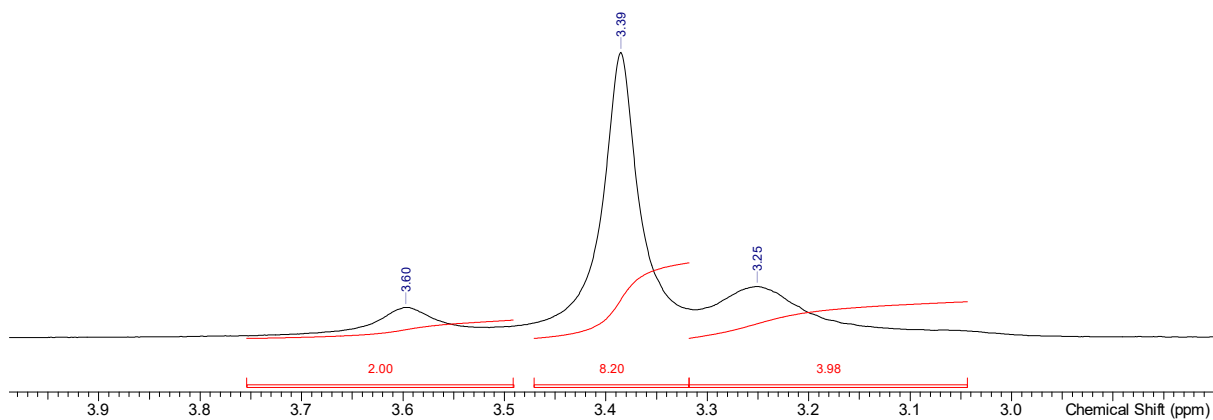


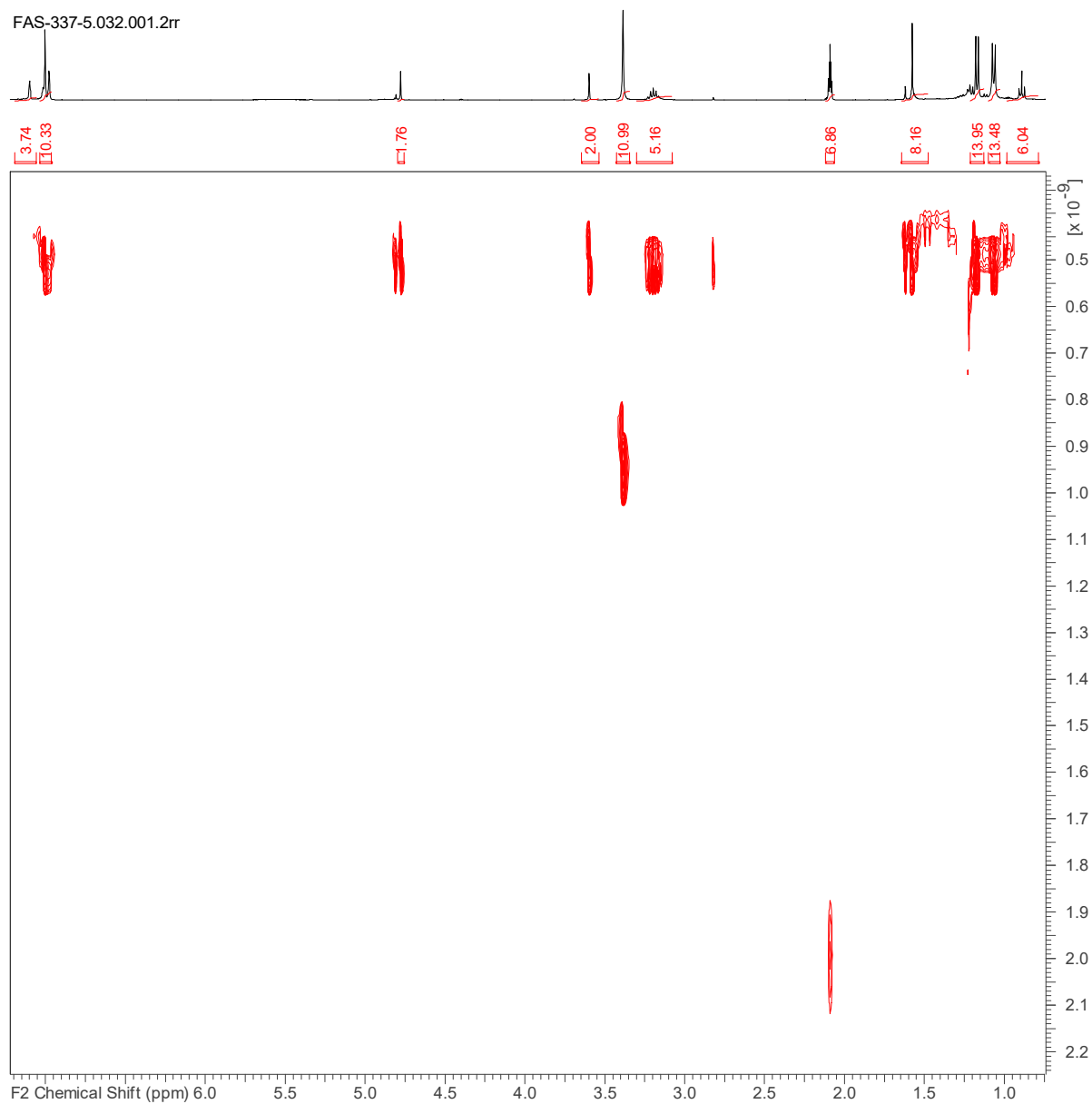**Figure S17.** $^1$H DOSY NMR spectrum (400 MHz) of **(BODDI)(MgEt)$_2$*dx$_2$** in toluene-d$_8$ (solvent peaks at 2.09, 6.98, 7.00, and 7.09 ppm) at 297 K.

13

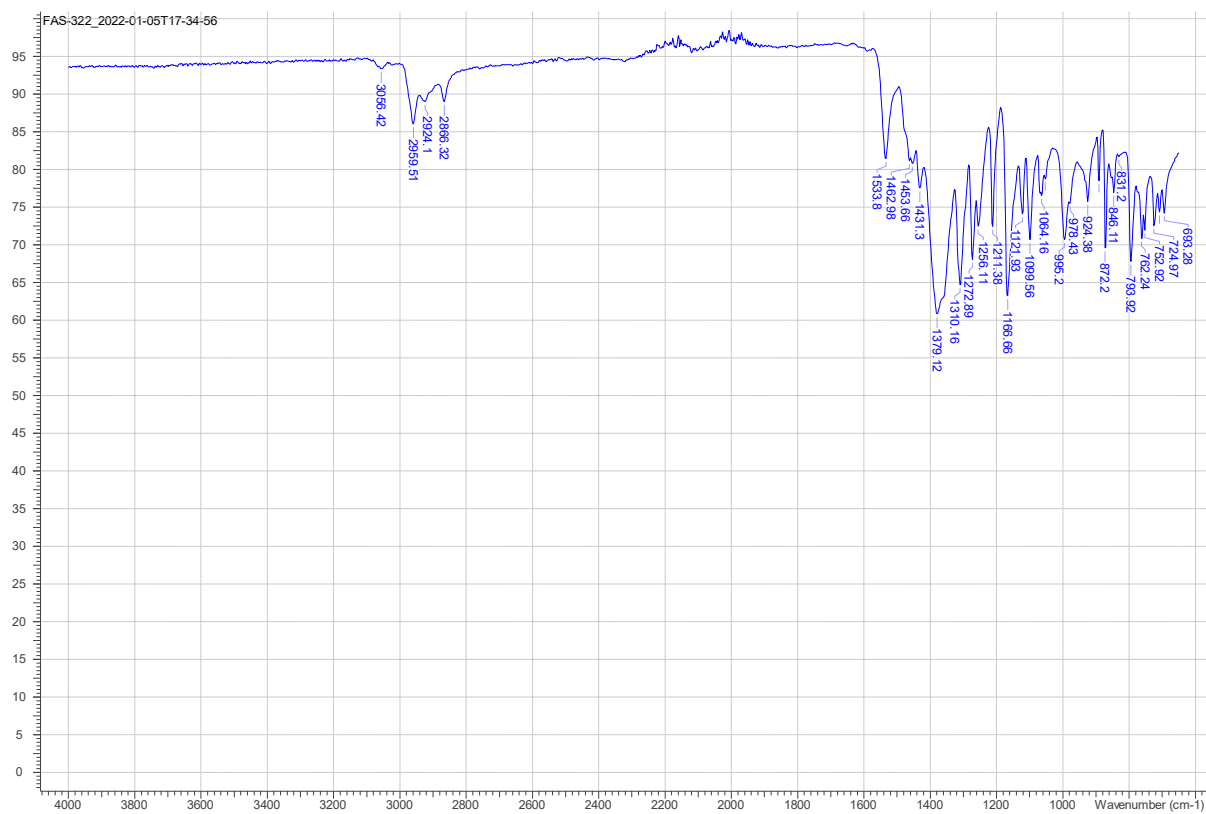**Figure S18.** ATR-IR (diamond) spectrum of **(BODDI)$_2$(MgH)$_4$*dx**.

## Computational details

All quantum chemical calculations determining structural and electronic properties of the tetranuclear magnesium hydride cluster **(BODDI)$_2$(MgH)$_4$** were obtained by the Gaussian 16 program package[8]. The fully relaxed singlet ground state equilibrium geometry of **(BODDI)$_2$(MgH)$_4$** was obtained at the density functional level of theory (DFT) by means of the B3LYP hybrid functional[9] and def2-SVP basis sets[10] for all atoms. The D3 version of Grimme's dispersion correction with the Becke-Johnson damping function was applied to account for dispersion effects.[11] Effects of interaction with a solvent (toluene: $\varepsilon$ = 2.374, n = 1.497) were taken into account by the solute electron density (SMD) variant of the integral equation formalism of the polarizable continuum model (equilibrium procedure).[12] A vibrational analysis was carried out to verify that a minimum on the 3N-6-dimensional potential-energy (hyper)surface (PES) was obtained. As shown very recently in a joint synthetic-spectroscopic-theoretical investigation for a structurally related BODDI-Al(III)-based chromophore, this computational setup allows to provide an unambiguous description of structural and of electronic ground state properties for this class of BODDI-based main group coordination compounds.[13]

Subsequently, the electronic structure, with particular emphasis on the tetranuclear magnesium hydride cluster, was evaluated by means a natural bond orbital (NBO) analysis. The 2e-stabilization ($\Delta E^{(2)}$) of the $i^{\text{th}}$ donor NBO by means of perturbative mixing with the $j^{\text{th}}$ acceptor NBO was obtained by the respective orbital energies (*i.e.*, $\varepsilon_i$ and $\varepsilon_j$), their orbital overlap ($F_{ij}$), and the occupation of the donor orbital ($q_i$):

$$\Delta E^{(2)} = \frac{q_i \cdot |F_{ij}|^2}{(\varepsilon_j - \varepsilon_i)} \quad .$$

Furthermore, the Wiberg bond indices (WBIs),[14] referring to the average number of electron pairs shared by two atoms centers, were calculated. The topology of the electronic bonds was studied based on an atoms in molecules charge analysis, i.e., Bader analysis,[15] performed using the Multiwfn package[16]. Finally, the nature of the coordination environment in the vicinity of $\mu_4$-hydrid was analyzed in-depth using the localized orbital locator (LOL)[17] as well based on a non-covalent interaction (NCI) analysis.[18]

The xyz coordinates of the optimized molecule are available free of charge via the open repository Zenodo.[19]

## References

[1]   a) S. D. Allen, D. R. Moore, E. B. Lobkovsky, G. W. Coates, *J. Organomet. Chem.* **2003**, *683*, 137; b) R. Fischer, D. Walther, G. Gebhardt, H. Görls, *Organometallics* **2000**, *19*, 2532.

[2]   COLLECT, Data Collection Software; Nonius B.V., Netherlands, **1998**.

[3]   „Processing of X-Ray Diffraction Data Collected in Oscillation Mode": Z. Otwinowski, W. Minor in C. W. Carter, R. M. Sweet (eds.): *Methods in Enzymology, Vol. 276, Macromolecular Crystallography, Part A*, pp. 307-326, *Academic Press*, **1997**.

[4]   SADABS 2.10, Bruker-AXS inc., **2002**, Madison, WI, U.S.A

[5]   G.M. Sheldrick, *Acta Cryst.* **2008**, *A64*, 112.

[6]   G.M. Sheldrick, *Acta Cryst.* **2015**, *C71*, 3.

[7]   O.V. Dolomanov, L.J. Bourhis, R.J. Gildea, J.A.K. Howard, H. Puschmann, *J. Appl. Cryst.* **2009**, *42*, 339.

[8]   Gaussian 16, Revision C.01, M. J. Frisch, G. W. Trucks, H. B. Schlegel, G. E. Scuseria, M. A. Robb, J. R. Cheeseman, G. Scalmani, V. Barone, G. A. Petersson, H. Nakatsuji, X. Li, M. Caricato, A. V. Marenich, J. Bloino, B. G. Janesko, R. Gomperts, B. Mennucci, H. P. Hratchian, J. V. Ortiz, A. F. Izmaylov, J. L. Sonnenberg, D. Williams-Young, F. Ding, F. Lipparini, F. Egidi, J. Goings, B. Peng, A. Petrone, T. Henderson, D. Ranasinghe, V. G. Zakrzewski, J. Gao, N. Rega, G. Zheng, W. Liang, M. Hada, M. Ehara, K. Toyota, R. Fukuda, J. Hasegawa, M. Ishida, T. Nakajima, Y. Honda, O. Kitao, H. Nakai, T. Vreven, K. Throssell, J. A. Montgomery, Jr., J. E. Peralta, F. Ogliaro, M. J. Bearpark, J. J. Heyd, E. N. Brothers, K. N. Kudin, V. N. Staroverov, T. A. Keith, R. Kobayashi, J. Normand, K. Raghavachari, A. P. Rendell, J. C. Burant, S. S. Iyengar, J. Tomasi, M. Cossi, J. M. Millam, M. Klene, C. Adamo, R. Cammi, J. W. Ochterski, R. L. Martin, K. Morokuma, O. Farkas, J. B. Foresman, D. J. Fox, Gaussian, Inc., Wallingford CT, **2016**.

[9]   a) C. Lee, W. Yang, and R. G. Parr, *Phys. Rev. B* **1988**, *37*, 785; b) A. D. Becke, *J. Chem. Phys.* **1993**, *98*, 5648.

[10]  a) F. Weigend, R. Ahlrichs, *Phys. Chem. Chem. Phys.* **2005**, *7*, 3297; b) F. Weigend, *Phys. Chem. Chem. Phys.*, **2006**, *8*, 1057.

[11]  S. Grimme, S. Ehrlich, L. Goerigk, *J. Comp. Chem.* **2011**, *32*, 1456.

[12]  a) B. Mennucci, C. Cappelli, C. A. Guido, R. Cammi, J. Tomasi, *J. Phys. Chem. A* **2009**, *113*, 3009; b) A. V. Marenich, C. J. Cramer, D. G. Truhlar, *J. Phys. Chem. B* **2009**, *113*, 6378.

[13]  F. L. Portwich, Y. Carstensen, A. Dasgupta, S. Kupfer, R. Wyrwa, H. Görls, C. Eggeling, B. Dietzek, S. Gräfe, M. Wächtler, R. Kretschmer, *Angew. Chem. Int. Ed.* **2022**, *61*, e202117499.

[14]  K. B. Wiberg, *Tetrahedron*, **1968**, *24*, 1083.

[15]  a) R. F. W. Bader, P. M. Beddall, *J. Chem. Phys.* **1972**, *56*, 3320; b) R. F. W. Bader, P. L. A. Popelier, T. A. Keith, *Angew. Chem. Int. Ed. Engl.* **1994**, *33*, 620.

[16]  T. Lu, F. Chen, *J. Comp. Chem.* **2012**, *33*, 580.

[17]  H.L. Schmider, A.D. Becke, *J. Mol. Struc. Theochem.* **2000**, *527*, 51.

[18]  E. Pastorczak, C. Corminboeuf, *J. Chem. Phys.* **2017**, *146*, 120901.

[19]  https://doi.org/10.5281/zenodo.778.